Available online at www.sciencedirect.com
SCIENCE DIRECT®
Agricultural and Forest Meteorology 117 (2003) 173–192
AGRICULTURAL AND FOREST METEOROLOGY
www.elsevier.com/locate/agrformet

Partitioning of water flux in a Sierra Nevada ponderosa pine plantation

M.R. Kurpius [a,*], J.A. Panek [a], N.T. Nikolov [b], M. McKay [a], A.H. Goldstein [a]

[a] *Department of Environmental Science, Policy and Management, University of California, Berkeley, CA, USA*
[b] *US Geological Survey, Fort Collins, CO, USA*

Received 4 February 2002; received in revised form 7 January 2003; accepted 20 January 2003

Abstract

The weather patterns of the west side of the Sierra Nevada Mountains (cold, wet winters and hot, dry summers) strongly influence how water is partitioned between transpiration and evaporation and result in a specific strategy of water use by ponderosa pine trees (*Pinus ponderosa*) in this region. To investigate how year-round water fluxes were partitioned in a young ponderosa pine ecosystem in the Sierra Nevada Mountains, water fluxes were continually measured from June 2000 to May 2001 using a combination of sap flow and eddy covariance techniques (above- and below-canopy). Water fluxes were modeled at our study site using a biophysical model, FORFLUX. During summer and fall water fluxes were equally partitioned between transpiration and soil evaporation while transpiration dominated the water fluxes in winter and spring. The trees had high rates of canopy conductance and transpiration in the early morning and mid-late afternoon and a mid-day depression during the dry season. We used a diurnal centroid analysis to show that the timing of high canopy conductance and transpiration relative to high vapor pressure deficit (D) shifted with soil moisture: during periods of low soil moisture canopy conductance and transpiration peaked early in the day when D was low. Conversely, during periods of high soil moisture canopy conductance and transpiration peaked at the same time or later in the day than D. Our observations suggest a general strategy by the pine trees in which they maximize stomatal conductance, and therefore carbon fixation, throughout the day on warm sunny days with high soil moisture (i.e. warm periods in winter and late spring) and maximize stomatal conductance and carbon fixation in the morning through the dry periods. FORFLUX model estimates of evaporation and transpiration were close to measured/calculated values during the dry period, including the drought, but underestimated transpiration and overestimated evaporation during the wet period.

Keywords: Drought stress; Transpiration; Conductance

1. Introduction

The west side of the Sierra Nevada is characterized by a Mediterranean climate, with cold, wet winters and hot, dry summers. These weather patterns impose restrictions on transpiration rates: in winter water is abundant but near-freezing temperatures are limiting while in summer sunlight and temperatures are optimal but water is limiting. Given these constraints, how water is partitioned, i.e. transpired or evaporated from

* Corresponding author. Present address: Department of Forestry, 321 Richardson Hall, Oregon State University, Corvallis, OR 97331-5752, USA. Tel.: +1-541-737-8473; fax: +1-510-643-5098.
E-mail addresses: meredith.kurpius@orst.edu (M.R. Kurpius), jpanek@nature.berkeley.edu (J.A. Panek), nikolov10@attbi.com (N.T. Nikolov), megan@nature.berkeley.edu (M. McKay), ahg@nature.berkeley.edu (A.H. Goldstein).

0168-1923/03/$ – see front matter
doi:10.1016/S0168-1923(03)00062-5

surfaces, is critical in west side Sierra Nevada forests. Ponderosa pine (*Pinus ponderosa*) is the most abundant conifer west of the Rocky Mountains and is a dominant tree species in the mixed-conifer forests of the Sierra Nevada Mountains (SNEP, 1996). Given the extent of the Sierra Nevada forests and abundance of ponderosa pine, the specific strategy of water use by this species is of particular interest.

Modeling gas exchange in ecosystems that experience seasonal drought stress has proven to be a difficult challenge (Law et al., 2000). Since it is prohibitively expensive to measure water fluxes at a multitude of sites, models are an important tool in understanding and predicting how water is partitioned in different ecosystems. This is especially true given the need to understand how vegetation will respond to projected scenarios of climate change. Nikolov (Nikolov, 1997a,b; Nikolov et al., 1995) developed FORFLUX, a biophysical model, to study the exchange of water vapor, CO_2, O_3, and energy between terrestrial ecosystems and the atmosphere. The model mechanistically couples major ecosystem processes controlling the flows of carbon and water. The FORFLUX model has been used with relative success in a subalpine forest (Zeller and Nikolov, 2000), lodgepole pine (*Pinus contorta*), limber pine (*Pinus flexilis*), and quaking aspen (*Populus tremuloides*) (Nikolov et al., 1995), along with cotton and grapevine fields (Nikolov, 1997a). The model is unique in that it simulates the feedback between canopy transpiration rate and stomatal sensitivity to drought and freezing, and uses this information to constrain conductance. These features make FORFLUX a promising model for ecosystems that experience seasonal drought stress. However, the ability of this model to predict trace gas exchange in a drought-stressed forest ecosystem has remained untested.

To investigate how year-round water fluxes were partitioned in a young ponderosa pine ecosystem in the Sierra Nevada Mountains, we continually measured water fluxes from June 2000 to May 2001 using two methods: (1) measuring sap flow in trees; and (2) using sub-canopy and above-canopy eddy covariance techniques to determine soil and total canopy water flux, respectively. We calculated canopy conductance from sap flow data using an inverse Penman–Monteith equation. Environmental variables including air temperature, soil moisture, vapor pressure deficit, and photosynthetically active radiation were measured continuously. We modeled water fluxes at our study site using FORFLUX. Finally, we conducted a diurnal centroid analysis of transpiration, canopy conductance, and vapor pressure deficit to investigate how water status affects the diurnal patterns of transpiration and canopy conductance.

2. Methods

2.1. Site description

The Blodgett Forest Ameriflux field site was established in May 1997 in a ponderosa pine plantation in the Sierra Nevada Mountains. The ponderosa pine plantation is owned by Sierra Pacific Industries, located adjacent to Blodgett Forest Research Station, a research forest of the University of California at Berkeley near Georgetown, CA (38°53′42.9″ N, 120°37′57.9″ W) at 1300 m elevation. A 12-m tower was erected on the site in order to make measurements above the canopy (see Goldstein et al., 2000 for detailed map of tower surroundings). The forest upwind of the tower, comprising the sampled footprint, is a homogeneous stand of trees dominated by ponderosa pine (*P. ponderosa*). During the measurement period, the trees were 8–9 years old and 5–6 m high and had a stand density of ∼600 trees ha^{-1}. The stand also includes individuals of Douglas fir (*Psuedotsuga menziesii*), white fir (*Abies concolor*), incense cedar (*Calcedrus decurrens*), sugar pine (*Pinus lambertiana*) and black oak (*Quercus kelloggii*). Shrubs were removed in May 1999 and roughly two-thirds of the trees were removed in May 2000 based on typical thinning practices by Sierra Pacific Industries. The leaf area index (LAI) for this site was estimated to be 2.2 following the tree thinning. The percent coverage by trees, shrubs, forbs, bare, and debris were 24, 25, 6, 11, and 34%, respectively. A ponderosa pine plantation that is 7–8 years older is located 200 m to the southwest of the measurement site upwind of the tower during the day. Two independent model estimates of the tower footprint both indicate that roughly 90% of the footprint was within the young plantation (200 m of the tower) during the daytime (Baker et al., 1999; Goldstein et al., 2000).

The site is characterized by a Mediterranean climate, with the majority of precipitation falling between September and May and very little rain in the summer. Since 1961, annual precipitation has averaged 163 cm (minimum 67.3 cm, maximum 276 cm, S.D. 52.1 cm). Summer temperatures typically range from 14 to 27 °C, and winter temperatures typically range from 0 to 9 °C (data from Blodgett Forest Archives). Trees generally break bud in mid-May to early June and set bud late July to early August. The predominant daytime airmass trajectory at the site comes upslope from the Sacramento Valley. The site receives nighttime air downslope from the Sierra Nevada Mountains to the east. The soil is in the Cohasset series and was formed in material weathered from andesitic lahar (R. Heald, personal communication).

Infrastructure for the canopy-scale flux measurements included the measurement tower (Upright Inc.), two temperature controlled instrument buildings, and an electrical generation system powered by a diesel generator. The measurement tower was placed toward the eastern side of the plantation to maximize the ponderosa pine plantation fetch during the day. The generator was located 500 ft to the northwest of the tower, as far outside of the major airflow paths as possible. Hydrocarbon measurements at the site indicated that exhaust from the generator affected our measurements less than 5% of the time and contamination occurred only at night (Lamanna and Goldstein, 1999).

2.2. Sap flow measurements

Sap flow was monitored using the heat-ratio method (Burgess et al., 2001) from June 1, 2000 to May 31, 2001. Units comprising two thermistor probes and one heater probe were inserted radially into the sapwood of 8–9-year-old ponderosa pine trees at 1.3–1.4 m above the ground (Fig. 1). For each sensor set, a 30 mm long thermistor probe was placed 6 mm above and 6 mm below the 30 mm long heater probe. Holes for the 1.3 mm

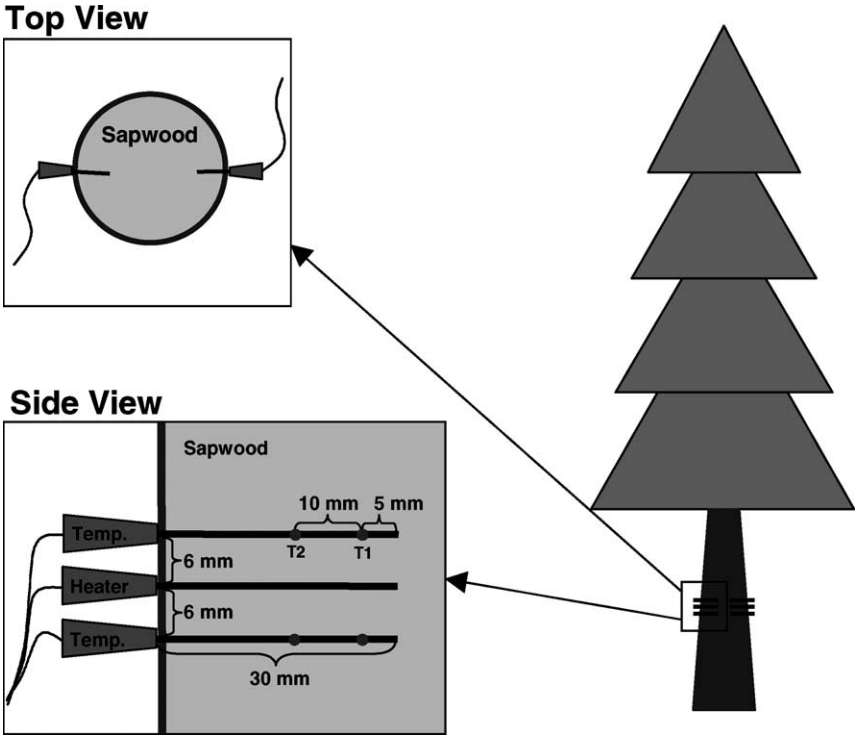

Fig. 1. Schematic showing orientation and placement of sap velocity probes. The side view shows the two temperature probes, each with two thermocouple junctions (T1 and T2), and the heater probe between the temperature probes.

wide probes were carefully drilled with 1.4 mm diameter bits, aligned to the correct spacing by a 15 mm thick jig. The probes were coated with petroleum jelly before being inserted into the holes. Each thermistor measured temperature at two distances along the probe—5 and 15 mm from the inner end of the probe. Once the sensors were inserted, a 15–20 cm wide collar of reflective insulation was placed around the tree where the sensors were placed to prevent direct solar radiation on the exposed portions of the sensors.

Eight sensor sets were deployed, one on the east side and one on the west side, in each of four trees (Fig. 1). The trees sampled were chosen to represent the size distribution of the stand. Since this was a plantation that had recently been thinned, the size distribution was very uniform. There were few trees with DBH less than 10 cm or greater than 20 cm. Based on measurements of 83 trees taken in a 10 m × 180 m transect, 90% of the sapwood area of the stand was made up of trees with DBH between 10.8 and 20 cm. The mean DBH for this 90% was 14.1 cm ± 2.3 cm (one standard deviation). Sap velocity measurements from individual sensors were within 10% of the mean for all trees, indicating fairly uniform sap flow among different trees and on different sides of trees. Given the low sample size in this study it is possible that the sap flow measurements in the trees measured are not truly representative of the entire stand within the eddy covariance footprint. While a larger sample of trees would have been preferable, others have found that smaller sample sizes are adequate for a uniform stand with trees that are regularly spaced (cf. Granier, 1987; Hatton et al., 1990; Kline et al., 1976; Saugier et al., 1997).

Three tree cores were taken every 2 weeks using an increment borer to determine sapwood fresh weight, sapwood oven-dried weight, water content and wood volume. Trees of various sizes were harvested and were used to determine depth of bark and cambium, and sapwood area. Total sapwood was calculated as:

$$\text{total sapwood area} = \pi(\text{under bark radius})^2 - \pi(\text{under bark radius} - \text{heartwood boundary})^2 \quad (1)$$

It was determined that sapwood comprised almost all the cross-sectional area inside the cambium. Inner (5 mm from inner tip, 25 mm from bark) and outer (15 mm from inner tip, 15 mm from bark) temperature readings were used to capture the spatial variability of inner versus outer sapwood. Outer sapwood area was calculated as:

$$\text{outer sapwood area} = \pi(\text{under bark radius})^2 - \pi(\text{under bark radius} - 20\,\text{mm})^2 \quad (2)$$

Inner sapwood area was calculated as:

$$\text{inner sapwood area} = \text{total sapwood area} - \text{outer sapwood area} \quad (3)$$

In terms of sapwood area represented, this thermocouple spacing provides 50% for inner and outer sapwood for trees with DBH of 14.3 cm. The ratio of outer:inner sapwood for the sample trees was 1.11, 0.75, 1.0, and 0.8. Although longer probes would have provided more detailed measurements of the inner tree, the accuracy of this measurement technique is highly dependent on proper alignment within the tree and can become compromised by longer probes. Given the size of the trees in our plot we used a thermocouple spacing that would both adequately characterize the cross-sectional variability and minimize probe alignment errors.

Corrections were applied for: vertical probe misalignment, adjustment for correct thermal diffusivity (Becker and Edwards, 1999), wound effects, and radial and circumferential variation in rates of sap flow (Burgess et al., 2001). Further, the sap velocity measurements were adjusted to account for volumetric wood and water contents (Hatton et al., 1995). Overall, corrections ranged from 1 to 5% depending mainly on probe alignment. Burgess et al. (2001) found the heat-ratio method to be less prone to unexplained variation than the traditional compensation heat-pulse method. For a full description of errors and reliability associated with the heat-ratio method, see Burgess et al. (2001).

Stand transpiration (E_t, mm h^{-1} or mm day^{-1}) was estimated from $E_t = J \times S$, where J is the sap flux density ($mm^3\,mm^{-2}\,h^{-1}$) and S is the cross-sectional sapwood area per ground area ($m^2\,m^{-2}$). Sap flux density is the mean sap flow averaged by the mean sapwood area (see Clearwater et al., 1999; Granier and

Loustau, 1994; Teixeira Filho et al., 1998). It was necessary to account for a 1/2 h time lag between when sap began moving through the trunk and when it was transpired. We determined the lag-time by matching sap flow water flux measurements with above-canopy water flux measurements.

Scaling sap flow measurements from the measurement point to the tree and then from the tree to the stand can be problematic. The two biggest issues in scaling sap flow measurements are in non-uniform sapwood and non-uniform stand properties. Sap flux density can vary spatially within the conducting wood (see Dye et al., 1991; Hatton and Vertessy, 1989, 1990; Lassoie et al., 1977; Miller et al., 1980; Olbrich, 1991). Sapwood xylem of plantation trees which are evenly spaced are known to be fairly regular (Kostner et al., 1998). The distribution of sensors within and around the sample trees showed very little variation in sap flow based on depth or aspect. Errors from within stand variability can be reduced by stratifying trees within the stand by size class (Hatton et al., 1995; Kostner et al., 1998). Since we were working in a very uniform plantation of even-aged and evenly distributed trees, these scaling issues should be minimized.

A rearranged Penman–Monteith equation was used to calculate canopy resistance (r_c) (Monteith and Unsworth, 1990; Shuttleworth et al., 1984):

$$r_c = \left\{ \left(\Delta' \frac{\lambda}{c_p} \right) \beta - 1 \right\} r_a + \frac{\rho\lambda\{q_w(T) - q\}}{\lambda E} \quad (4)$$

where Δ' is the slope of the saturated specific humidity curve at mean air temperature ($g\,kg^{-1}\,K^{-1}$), λ is the latent heat of vaporization ($J\,g^{-1}$), c_p is the specific heat of air at constant pressure ($J\,kg^{-1}\,K^{-1}$), β is the Bowen ratio (dimensionless), r_a is the aerodynamic resistance ($s\,m^{-1}$), ρ is the density of dry air ($kg\,m^{-3}$), $q_w(T)$ is the saturated specific humidity at temperature T ($g\,kg^{-1}$), q is the specific humidity at height z ($g\,kg^{-1}$), λE = latent heat flux ($J\,s^{-1}\,m^{-2}$). Canopy conductance (g_c) was calculated as the inverse of canopy resistance.

2.3. Eddy covariance and meteorological measurements

Above-canopy latent heat flux was measured continuously using an infrared CO_2/H_2O analyzer (Li-Cor 6262, Li-Cor, Inc.) and a three-axis sonic anemometer system (SATI/3Sx, ATI, Inc.) mounted on a tower at 12 m above the ground. The above-canopy latent heat fluxes were used to determine evapotranspiration (E). Sub-canopy water flux measurements were made during a subset of the measurement period (August 23, 2000–September 30, 2000) using a similar system as that used for above-canopy flux measurements except that the sonic anemometer was mounted on a separate mini-tower at 2 m above the ground in an open area of roughly 20 m^2 which we chose to be representative of the sub-canopy environment (bare and debris made up 45% of ground coverage in the stand). Most of the trees less than 4–5 m tall were removed in the thinning, resulting in very little leaf area below the measurement height. Therefore, we expect our measurements to give an estimate of ground evaporation at our site.

Half-hour files of raw 10 Hz data were logged to a computer at the site. Ten Hz flux data were processed using RAMF (Chambers et al., 1997) (Routinen zur Auswertung Meteorologicscher Forschungsflüge, Routines for the Processing of Meteorological Research Flights) software routines which were developed at the Flinders Institute for Atmospheric and Marine Sciences, Flinders University of South Australia. RAMF was designed to operate with high resolution meteorological and turbulence data and is capable of handling large datasets. Half-hour data files generated using RAMF were imported into S-Plus for quality control, data management, statistical analysis, and graphing. S-Plus is a data analysis and statistical modeling program developed by Insightful Corp.

Corrections and adjustments were made to account for potential systematic errors in the eddy covariance fluxes. Adjustments were made for the time lag between sampling and instrument response and to align the vertical velocity measurement to normal to mean streamlines. The time lag between the sampling and instrument response was determined by maximizing the covariance between the vertical wind and H_2O concentration. The time lag was 5.0 s and was consistent throughout the measurement period. Errors may occur in the calculation of covariances because of inappropriate orientation of the vertical wind sensor. These potential errors due to misalignment of wind sensors with respect to the local mean streamline were eliminated by a three-dimensional coordinate rotation of the mean wind vectors (McMillen, 1988). The rotation angle needed to align the vertical

velocity measurement to normal to mean streamlines was typically 0.6°.

Systematic errors associated with the eddy covariance fluxes include damping of the high-frequency fluctuations by the closed path infrared gas analyzer and travel through the sampling tube, sensor separation between the vertical wind measurement and H_2O sample inlet, and the inability of the sonic anemometer to resolve fine-scale eddies in light winds. Errors due to sensor separation arise when the vertical wind measurement and gas inlet are not located at the same point in space. Damping of fluctuations in gas concentration occurs when air is passed through a tube to a closed path analyzer because of radial variation in streamwise air velocity and because of radial diffusion; the tube acts as a low-pass filter (Leuning and Judd, 1996). Errors due to sensor separation and damping of high-frequency eddies were corrected using spectral analysis techniques as outlined by Kaimal and Finnegan (1994) and Rissmann and Tetzlaff (1994). Using cospectral analysis (a means to characterize contributions to the covariance between two quantities as a function of frequency), it is possible to derive a scaling factor to correct a covariance estimate. Assuming that the observations of vertical wind (w) are reliable, a comparison of the "observed" normalized cospectra with a theoretically "correct" cospectra should indicate the effect of errors such as sensor separation and damping of high-frequency eddies. Since temperature measurements from sonic anemometers have high sampling frequency and accuracy, the normalized temperature cospectra is commonly used as a surrogate for the "correct" cospectra. Under ideal conditions, the shapes of the power spectra for $w'T'$ (sensible heat flux) and $w'H_2O'$ (latent heat flux) should be similar (Rissmann and Tetzlaff, 1994). Sensible heat flux can be considered the "ideal" flux; by comparing the power spectra of the sensible heat flux to those of the latent heat flux (the "less ideal" flux), errors due to sensor separation and damping of high-frequency eddies were assessed. Spectral analysis revealed an underestimation of latent heat flux of 11–13% (Goldstein et al., 2000). Correction factors for each half-hour were calculated and applied to the fluxes during the times when the sensible heat flux data were reliable. Additionally, spectral analysis indicated that fluxes were dominated by eddies with frequencies between 0.1 and 0.01 Hz. The inability of the sonic anemometer to resolve fine-scale eddies in light winds (such as at night) results in the inability to correct the latent heat flux data using spectral analysis techniques that assume $w'T'$ is the "correct" cospectrum. During the daytime, turbulence was typically strong enough to produce reliable measurements; however, nighttime flux measurements were less reliable. Therefore, the daytime latent heat fluxes were corrected using spectral techniques, but the correction based on spectral analysis was not applied to the nighttime data.

We calculated soil evaporation (E_s) as the difference between evapotranspiration (E) and transpiration (E_t), i.e. $E_s = E - E_t$ (Baldocchi et al., 1987; Saugier et al., 1997). Although we have tried to minimize errors in E and E_t we have likely not fully eliminated them. The result is that the calculation of E_s as $E - E_t$ will contain errors from both E and E_t. We therefore present $E - E_t$ as a coarse estimate of soil evaporation and recognize that it will contain some signal from canopy evaporation and shrub transpiration.

The meteorological measurements made pertaining to this work were: air temperature (HMP45C, Vaisala, Inc.) measured at 12 m, photosynthetically-active radiation (Q_p) (Q-7, Li-Cor, Inc.) measured at 12 m, precipitation (Model 385, Met One), and soil moisture at 10, 30, and 50 cm (CS615, Campbell Scientific, Inc.). Half-hour averages of air temperature, Q_p, rain, and soil moisture were recorded on a datalogger (CR10X, Campbell Scientific, Inc.). Vapor pressure deficit (D) was calculated as the difference between saturated and measured vapor pressure at ambient air temperature above the plantation. Pre-dawn and afternoon water potential was measured on one south-facing twig from each of 10 trees using a pressure bomb (Model 600 Pressure Chamber, PMS Instruments) on July 18, August 15, and August 29, 2000. Additionally, water potential measurements were made on the same days on 4 of the 10 trees at 07:50, 09:50, 11:50, and 13:50 Pacific Standard Time (PST).

2.4. Modeling

The FORFLUX model was used in this study because it is a multi-layer biogeochemical model designed to study diurnal and seasonal dynamics of all major fluxes of carbon and water in forest ecosystems (Nikolov, 1997a,b; Nikolov et al., 1995). The model consists of four interconnected modules: (1) a

leaf photosynthesis model (LEAFC3); (2) a canopy flux model; (3) a soil model of heat, water, and CO_2 transport; and (4) a snowpack model. Hourly values of evapotranspiration, transpiration, and soil evaporation were simulated.

The LEAFC3 module is a generic photosynthesis model that couples the leaf's major biochemical process with stomatal function and the energy- and mass-exchange mechanisms in the leaf boundary layer. The main components of the LEAFC3 module include: (1) leaf biochemical processes (based on Brooks and Farquhar, 1985; Collatz et al., 1991; Farquhar, 1988; Farquhar and Song, 1984; Farquhar and von Caemmerer, 1982; Farquhar et al., 1980; Harley et al., 1992; Sharkey, 1985); (2) stomatal conductance (based on Ball et al., 1987, 1988) with a modification to account for root hydraulic and chemical signaling on leaf stomatal aperture; (3) leaf boundary conductance (based on Campbell, 1977; Gates, 1980; Monteith and Unsworth, 1990); and (4) leaf energy balance which assumes that the total energy absorbed by a leaf is dissipated through latent and sensible heat fluxes, long-wave radiation, and metabolic storage (steady-state case).

The canopy flux module of FORFLUX predicts the exchange of CO_2 and water vapor between the above-ground portion of a vegetation stand and the atmosphere. Canopy photosynthesis and evapotranspiration are estimated by combining the LEAFC3 module with algorithms which simulate radiative transfer within the canopy, variation of foliage photosynthetic capacity with canopy depth, wind speed attenuation within the canopy, and rainfall interception by foliage elements. The soil module simulates the dynamics of moisture and temperature in the soil profile, soil-surface evaporation, and CO_2 efflux from soil due to root and microbial respiration. The transport of water and heat in soil is modeled employing physical principles and explicitly accounting for the effect of soil heterogeneity on field-scale fluxes. The FORFLUX soil model consists of two complementary parts: (1) a module that simulates the one-dimensional (vertical) flow of water and heat in a homogeneous soil column by combining Darcy's law with the continuity equation; and (2) an algorithm that employs observed probability distributions of soil hydraulic properties to characterize field spatial variability in terms of a number of independent soil columns with different hydraulic characteristics and the percent area occupied by them.

A novel aspect of this model is that it allows for simulation of the observed feedback between canopy transpiration rate and stomatal sensitivity to adverse conditions such as drought or freezing. For example, when the soil dries, a message is carried from the roots to the leaves via sap flow, causing partial stomatal closure. This in turn reduces root water extraction and slows down soil desiccation. This soil-canopy feedback is simulated in FORFLUX by a root–shoot communication algorithm that incorporates recent findings about hydraulic and chemical signaling in plants. Tardieu and Davies (1993a,b), and Tardieu et al. (1993) found that the sensitivity of stomatal conductance to ABA, the hormonal messenger for root status, increases exponentially with the fall in leaf water potential. A root–shoot communication algorithm was developed in FORFLUX to estimate the root signal emitted to leaf stomata based on the aforementioned work by Tardieu and Davies (1993a,b), and Tardieu et al. (1993). The root–shoot algorithm requires the canopy transpiration rate, the root interfacial conductance, soil water pressure head, the rooting depth, relative root water uptake, and three species-specific parameters and determines the field-averaged root signal. The field-averaged root signal is then incorporated into the Ball–Berry equation in the LEAFC3 module and is used to constrain stomatal conductance of all leaves in the canopy at a given time step.

The model was parameterized using data collected at the field site or assumed based on information in the literature. A list of the major parameters used in FORFLUX is presented in Table 1.

2.5. Diurnal centroid

Water status is expected to play an important role in water use for ponderosa pine, especially during the drought period. However, daily E_t rates at this site did not respond directly to decreasing soil moisture or to D increasing above 1.0 kPa, even when the trees were drought stressed. This does not necessarily indicate that water status is unimportant but rather that D and soil moisture cannot be considered independently. We hypothesize that low soil moisture causes a shift in peak water use to the morning because D is low at this time of day. To investigate the effect of soil moisture

Table 1
Parameter values used for the FORFLUX model

Parameter	Value	Units
Species parameters		
Maximum carboxylation velocity at the rate of 25 °C	41.5	$\mu mol\,m^{-2}\,s^{-1}$
Light-saturated potential rate of electron transport	87.1	$\mu mol\,m^{-2}\,s^{-1}$
Leaf activation energy for electron transport	36	$kJ\,mol^{-1}$
Coefficient controlling smoothness of transition between light and temperature limited potential rates of electron transport	0.7*	Dimensionless
Kinetic parameter for CO_2 at the rate of 25 °C	27×10^{-5}	$mol\,mol^{-1}$
Kinetic parameter for O_2 at the rate of 25 °C	0.41	$mol\,mol^{-1}$
PPFD light loss factor	0.48*	Decimal fraction
Ball–Berry stomatal sensitivity to relative humidity and CO_2	7.4	Dimensionless
Ball–Berry empirical constant for stomatal conductance	0.21	$mol\,m^{-2}\,s^{-1}$
Needle diameter	0.001	m
Shoot diameter	0.07	m
Nighttime temperature minimum threshold	3*	°C
Water stress root conductance parameter A	1.9×10^{-5}*	$mm\,h^{-1}$
Water stress root conductance parameter B	2.7×10^{-2}*	$mm\,h^{-1}$
Water stress root conductance parameter C	0.014*	$mm\,h^{-1}$
Root signal parameter A	2*	$\mu mol\,kg\,m^{-6}\,h^{-1}$
Root signal parameter B	30*	m^{-1}
Root signal parameter C	0.25*	$kg\,m^{-2}\,h^{-1}$
Critical temperature for root conductance	4*	°C
Leaf reflectance in the visible wavelength	0.09*	Decimal fraction
Leaf transmittance in the visible wavelength	0.06*	Decimal fraction
Leaf reflectance in the near infrared wavelength	0.52*	Decimal fraction
Leaf transmittance in the near infrared wavelength	0.35*	Decimal fraction
Site parameters		
Total stand leaf area index	2.2	$m^2\,m^{-2}$
Canopy mean inclination angle	57.4*	°
Canopy foliage clumping index	0.73	Dimensionless
Above-ground live sapwood N content	3.2*	$g\,m^{-2}$
Ambient atmospheric CO_2 concentration	370	$\mu mol\,mol^{-1}$
Soil bulk density (at 15 cm)	0.8	$kg\,m^{-3}$
Soil sand content (% of dry weight)	36	%
Soil clay content (% of dry weight)	28	%
Soil organic C content (% of dry weight)	3	%
Volumetric soil rock content (% of volume)	25	%
Total soil depth	3	m
Rooting depth	3*	m
Visible soil reflectance	0.24*	Decimal fraction
Near infrared soil reflectance	0.3*	Decimal fraction
Water table presence at soil bottom (Y/N)?	N*	
Initial snowpack depth	0	m
Initial snowpack density	0	m
Initial top-soil moisture content	75	% of field capacity
Initial bottom-soil moisture content	100*	% of field capacity
Mean annual air temperature	10.7	°C
Mean annual air temperature amplitude	3	°C
Wind speed measurement height	12	m

An asterisk indicates the value was not measured and was assumed or obtained from the literature.

on the diurnal pattern of water use relative to D we used a diurnal centroid analysis to compute the diurnal centroids (C_g) of E_t, g_c, and D. The diurnal centroid is calculated as:

$$C_{g\,x} = \frac{\sum_{t=1}^{48} X(t)t / \sum_{t=1}^{48} X(t)}{2} \quad (5)$$

where $C_{g\,x}$ is the diurnal centroid for variable x (in units of hours), t is the half-hour period of the day, and $X(t)$ is the value of E_t or D during half-hour period t (see Wilson et al., 2003). The division by 2 converts $C_{g\,x}$ from half-hour period of day to hour of day. We were primarily interested in daytime patterns so t was summed over half-hours when $Q_p > 0$. The diurnal centroid represents a mean time, weighted by variable x and indicates whether higher values are shifted towards the morning ($C_{g\,x} < 12$ h) or towards the afternoon ($C_{g\,x} > 12$ h).

3. Results

3.1. Seasonal patterns

3.1.1. Climate

Summer 2000 was generally sunny, warm, and dry (Fig. 2) with very little rain. Data from the year prior to the measurement period (June 1999–May 2000) show that the total yearly precipitation was 127 cm: this was 78% of normal rainfall (based on rainfall averages since 1961). Daytime mean soil moisture was 25–30% within the top 50 cm and steadily decreased. The minimum soil moisture levels were 11.8, 16.3, and 18.3% for 10, 30, and 50 cm, respectively. It became cooler and wetter as fall progressed with the main rainy season beginning in mid-October 2000. During this period soil moisture increased to 30–35% in the top 50 cm. Cold and wet conditions continued into the winter with low air temperatures, D and Q_p, and high soil moisture. Daytime mean temperatures generally remained between 0 and 10 °C during the winter with a minimum of −3 °C and a maximum of 15 °C. Spring 2001 had alternating cold, rainy periods and warm, sunny periods. By late April, the rainy season ended, resulting in increasing air temperatures, Q_p and D, and decreasing soil moisture.

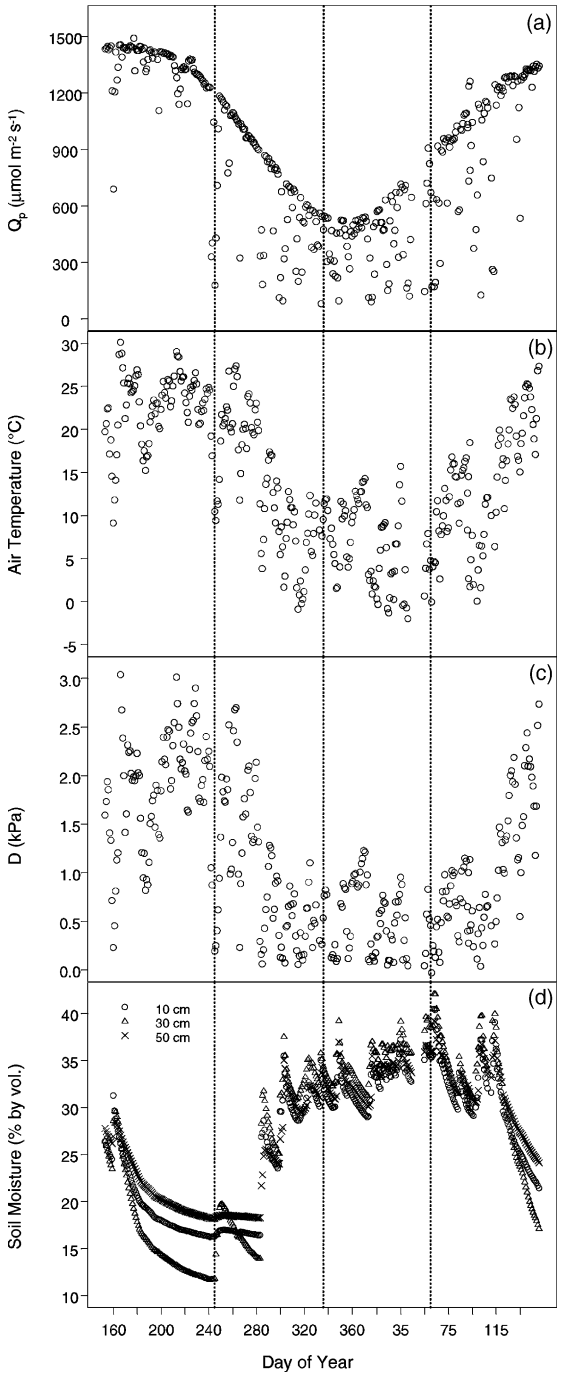

Fig. 2. Daytime mean (a) photosynthetically-active radiation (Q_p); (b) air temperature; (c) vapor pressure deficit (D); and (d) soil moisture. Beginning of timeline is June 1, 2000; end of timeline is May 31, 2001. From left to right the dotted vertical lines represent September 1, December 1, and March 1.

3.1.2. Water fluxes

Daily total evapotranspiration (E) increased in early summer to a maximum of ∼5 mm day^{-1} and then steadily decreased to 2–3 mm day^{-1} by mid-September (Fig. 3a). Mean daily total E (Table 2) for June 1–August 31 (days 153–244) was 3.23 mm day^{-1}. Daily total E continued to decrease through the fall to the yearly minimum of 0–1 mm day^{-1} by late November. A step-change in total daily E occurred in early October (day ∼280) which coincides with the onset of the rainy season. Mean daily total E for September 1 to November 31 (days 245–305) was 2.06 mm day^{-1}. Daily total E remained low (0–1 mm day^{-1}) through the winter with occasional values >1 mm day^{-1} when daytime mean air temperature exceeded 10 °C. Mean daily total E for December 1–February 28 (days 306–359) was 0.75 mm day^{-1}. Daily total E began increasing in early March, decreased to winter minimum values during a cold spell in late April, and then steadily climbed to 3–4 mm day^{-1} by the end of May. Mean daily total E for March 1–May 31 (days 60–151) was 1.77 mm day^{-1}. Modeled and measured daily total E (Fig. 3a) agreed well through the measurement period and were linearly related ($E_{\text{modeled}} = 0.82 \times E_{\text{measured}} + 0.36$, $r^2 = 0.82$, $P = 0.0000$).

Total daily transpiration (E_t) (Fig. 3b) measured with sap flow techniques was fairly constant (except during rain events) at 1.8–2.0 mm day^{-1} from early June until early August, when transpiration rates began to decline. Mean daily total E_t (Table 2) for June 1–August 31 (days 153–244) was 1.72 mm day^{-1} (53% of E). E_t rates steadily decreased from ∼2 mm day^{-1} in early August to ∼1 mm day^{-1} by early October (before the onset of the rainy period). Ponderosa pine trees are considered to be water stressed when pre-dawn water potential gets lower than −0.5 MPa: water potential measurements (Table 3) suggest that the ponderosa pine trees were not water stressed by July 18 but did become mildly water stressed by August 15. Daytime mean E_t was plotted against daytime mean D during June, July, August and September to examine how E_t responded to D during the dry season (Fig. 4). E_t increased curvilinearly with increasing D and then leveled off at ∼0.13 mm h^{-1} when D reached 1.0 kPa. E_t did not decrease at the highest levels of D. E_t rates further decreased with the onset of the rainy season in early

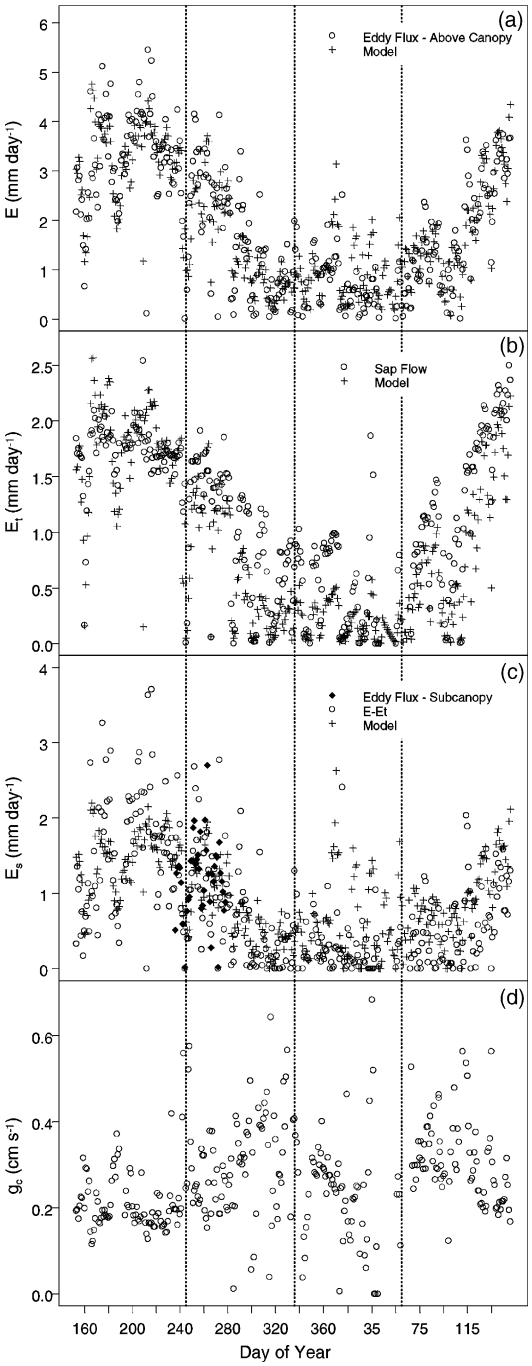

Fig. 3. Daily total (a) evapotranspiration (E); (b) transpiration (E_t); (c) soil evaporation (E_s); and (d) daytime mean canopy conductance (g_c). Beginning of timeline is June 1, 2000; end of timeline is May 31, 2001. From left to right the dotted vertical lines represent September 1, December 1, and March 1.

Table 2
Seasonal means (with standard deviation in parentheses) of daily total water fluxes

Days	Measured			Modeled		
	E	E_t	$E - E_t$	E	E_t	E_s
153–244	3.23 (1.01)	1.72 (0.28)	1.51 (0.81)	3.22 (0.81)	1.74 (0.48)	1.47 (0.40)
245–335	2.06 (1.12)	1.09 (0.57)	0.97 (0.69)	1.85 (0.87)	0.86 (0.54)	0.91 (0.45)
336–359	0.75 (0.55)	0.53 (0.43)	0.22 (0.37)	0.86 (0.54)	0.21 (0.15)	0.56 (0.49)
60–151	1.77 (1.08)	1.27 (0.68)	0.50 (0.51)	1.78 (1.02)	0.84 (0.63)	0.87 (0.48)

Table 3
Water potential (MPa) data for selected days during summer 2000

	Pre-dawn	07:50 PST	09:50 PST	11:50 PST	13:50 PST	Late afternoon
18 July	0.45 (0.01)	0.80 (0.14)	1.38 (0.12)	1.39 (0.14)	1.62 (0.80)	1.39 (0.10)
15 August	0.70 (0.04)	1.10 (0.13)	1.35 (0.20)	1.57 (0.07)	1.60 (0.10)	1.40 (0.08)
29 August	0.75 (0.05)		0.96 (0.06)	1.29 (0.09)	1.22 (0.13)	1.02 (0.05)

Pre-dawn and late afternoon measurements were done on 10 trees. Measurements at 07:50, 09:50, 11:50, and 13:50 PST were done on 4 of the 10 trees. Standard deviations are presented in parentheses.

October (day ∼280). However, the trees remained active, with daily total E_t of 0.5–1.0 mm day^{-1} when daytime mean air temperature exceeded 4–5 °C. Mean daily total E_t for September 1–November 31 (days 245–305) was 1.09 mm day^{-1} (53% of E). The trees remained active during warmer periods of the winter but the generally colder weather resulted in low (0–0.3 mm day^{-1}) total daily E_t through much of the winter. Mean daily total E_t for December 1–February 28 (days 306–359) was 0.53 mm day^{-1} (71% of E). Daily total E_t increased rapidly in spring, going from ∼0.5 mm day^{-1} in early March to the yearly maximum of 2.4 mm day^{-1} by the end of May. Mean daily total E_t for March 1–May 31 (days 60–151) was 1.27 mm day^{-1} (72% of E).

Modeled and measured daily total E_t (Fig. 3b) agreed fairly well through the measurement period and were linearly related ($E_{t\,modeled} = 0.95 \times E_{t\,measured} -$

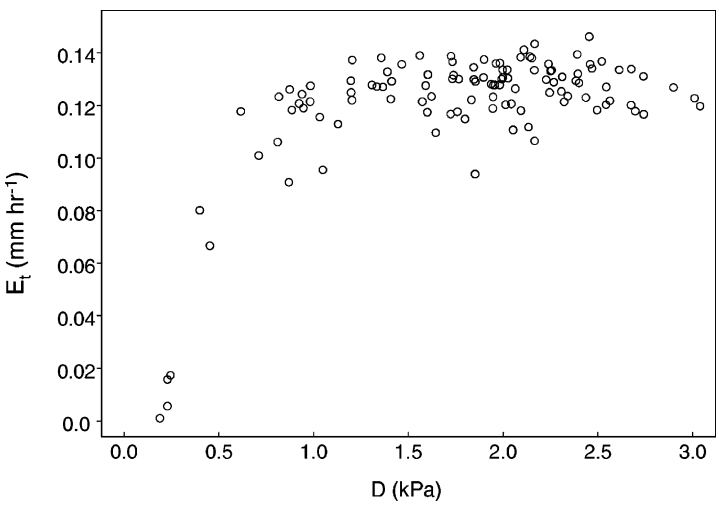

Fig. 4. Daytime mean transpiration (E_t) vs. daytime mean vapor pressure deficit (D).

0.19, $r^2 = 0.87$, $P = 0.0000$). The model performed best under warm, dry conditions (i.e. summer, early fall, and late spring), including when the trees were drought stressed. The modeled mean daily total E_t (1.74 mm day^{-1}) (Table 2) compared best to measured daily total E_t (1.72 mm day^{-1}) between June 1 and August 31 (days 153–244). The model underestimated E_t during the rainy season, predicting a mean daily total E_t of 0.21 mm day^{-1} between December 1 and February 28 (days 306–359) compared to the measured value of 0.53 mm day^{-1}.

Daily total calculated soil evaporation ($E - E_t$) (Fig. 3c) increased from ~1 mm day^{-1} in early June to 1.5–3 mm day^{-1} by mid-July and then gradually decreased through the summer. Mean daily total $E - E_t$ (Table 2) for June 1–August 31 (days 153–244) was 1.51 mm day^{-1} (47% of E). $E - E_t$ decreased from ~1 to 1.5 mm day^{-1} in mid-September to 0–0.5 mm day^{-1} by early December. Mean daily total $E - E_t$ for September 1–November 31 (days 245–305) was 0.97 mm day^{-1} (47% of E). $E - E_t$ remained low (0–0.5 mm day^{-1}) through the winter except for occasional sunny, warm periods when daytime mean air temperature exceeded 10 °C. Mean daily total $E - E_t$ for December 1–February 28 (days 306–359) was 0.22 mm day^{-1} (29% of E). $E - E_t$ increased slightly between early March and late April and then increased rapidly from ~0.5 mm day^{-1} in late April to ~1.2 mm day^{-1} by the end of March. Mean daily total $E - E_t$ for March 1–May 31 (days 60–151) was 0.50 mm day^{-1} (28% of E).

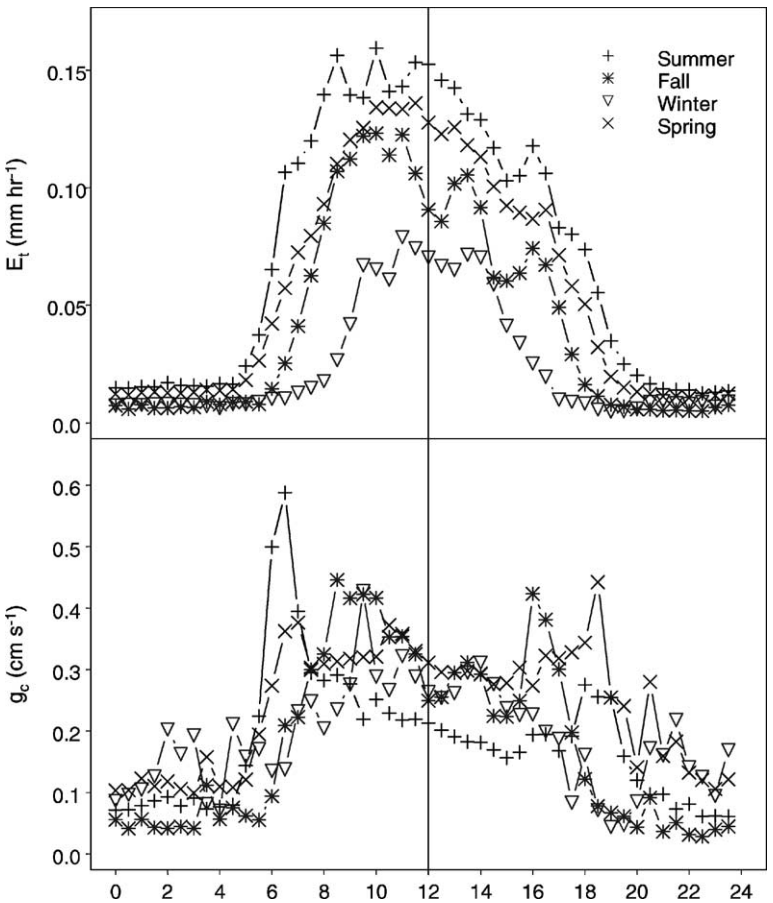

Fig. 5. Seasonal mean diurnal patterns for (a) transpiration (E_t), and (b) canopy conductance. Time of day is Pacific Standard Time (PST).

Modeled (E_s) and calculated ($E - E_t$) soil evaporation were weakly linearly related ($E_{s\,\text{modeled}} = 0.52(E - E_{t\,\text{calculated}}) - 0.47$, $r^2 = 0.50$, $P = 0.0000$). The modeled E_s was slightly lower than $E - E_t$ in the summer and fall (Table 2, Fig. 3c) and substantially higher than $E - E_t$ in the winter and spring. The estimate of soil evaporation obtained using eddy flux sub-canopy measurements (E_s) in the fall (Fig. 3c) agreed well in magnitude with both $E - E_t$ and modeled E_s; however, there was significant scatter in both the modeled and observed values, resulting in a poor correlation between sub-canopy measurements and $E - E_t$ and modeled values (r^2 for $E - E_t$ versus sub-canopy $E_s = 0.12$; r^2 for modeled E_s versus sub-canopy $E_s = 0.0015$).

3.1.3. Canopy conductance

Daytime mean canopy conductance (g_c) was 0.2–0.4 cm s^{-1} in the early summer and then decreased to 0.15–0.3 in mid-July (day ~190). As D dropped in early fall (day ~265) g_c increased slowly then jumped to 0.4 cm s^{-1} with the onset of the wet period in early October (day ~280). Canopy conductance (g_c) decreased in the winter and was highly variable with values generally between 0.05 and 0.3 cm s^{-1}. During spring, g_c had a range of 0.2–0.6 cm s^{-1}, maximizing when soil moisture and Q_p were high and air temperature and D were moderate.

3.2. Diurnal patterns

The diurnal patterns of E_t and g_c (Fig. 5) during summer and fall showed a morning peak, followed by an early afternoon depression and then partial recovery in the late afternoon. During spring, E_t had high values in the morning and slightly lower values in the afternoon but did not display the pronounced peak–depression–peak pattern seen in E_t in the summer and fall. The diurnal pattern of g_c in the spring had a small peak in the morning, sustained g_c during mid-day, and then a peak in late afternoon. During winter, E_t and g_c were low with diurnal patterns that were fairly unimodal.

The mean diurnal patterns of E_t and D for a month in the dry season (July) serve as an example of how to interpret the diurnal centroid (Fig. 6). In July, E_t increased rapidly with sunrise, reached a maximum before noon (09:00–10:00 PST), decreased until a mid-afternoon spike, and then decreased to near-zero by nightfall. D increased during the morning and early afternoon, maximized at 15:00–16:00 PST, and then decreased steadily through the afternoon. The mean diurnal centroid for E_t ($C_{g\,E_t}$) in July was 11.8 h (Fig. 6, Table 4), quantifying that E_t was centered slightly towards the morning. The diurnal pattern of D in July was centered towards the afternoon and had a mean diurnal centroid ($C_{g\,D}$) of 12.4 h. The mean

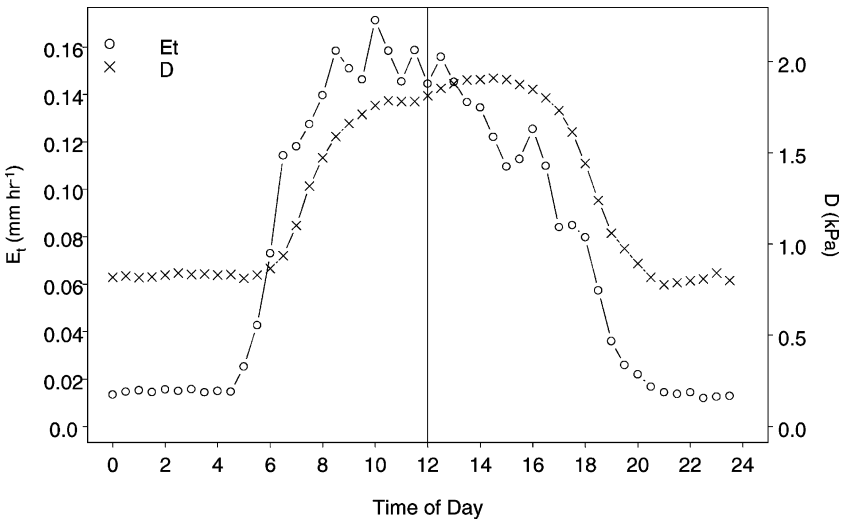

Fig. 6. Mean diurnal patterns for July 2000 for transpiration (E_t), and vapor pressure deficit (D). Time of day is Pacific Standard Time (PST).

Table 4
Mean monthly diurnal centroids for transpiration (C_{E_t}), canopy conductance (C_{g_c}), and vapor pressure deficit (C_D) for a month in the dry season (July) and a month in the wet season (January)

	$C^*_{E_t}$	$C^*_{g_c}$	C_D
July 2000	11.8 (1.1)	11.1 (0.8)	12.4 (0.8)
January 2001	12.4 (0.8)	12.5 (0.9)	12.1 (0.8)

Standard deviations are shown in parentheses. An asterisk indicates the mean diurnal centroids for July and January are significantly different from each other ($\alpha = 0.01$).

monthly diurnal centroids for E_t, g_c ($C_{g\,g_c}$), and D for a month in the dry season (July) and a month in the wet season (January) (Table 4) show that both E_t and g_c were centered significantly later in the day in January than in July ($P = 0.0004$ and 0.0000 for E_t and g_c, respectively). D was centered slightly later in July than in January (Table 4) but $C_{g\,D}$ for July was not significantly different statistically from $C_{g\,D}$ in January ($P = 0.7382$).

Weekly mean $C_{g\,D} - C_{g\,E_t}$ and $C_{g\,D} - C_{g\,g_c}$ were calculated and plotted against soil moisture at 10 cm (Fig. 7). The purpose of calculating both $C_{g\,D} - C_{g\,E_t}$ and $C_{g\,D} - C_{g\,g_c}$ was to examine the diurnal trends of E_t and g_c relative to D. The difference in diurnal centroid between two variables indicates how one variable is centered relative to the other. For example, in July $C_{g\,D} - C_{g\,E_t}$ was −0.6 h, indicating that $C_{g\,E_t}$ was centered 0.6 h ahead of $C_{g\,D}$. A negative value of $C_{g\,D} - C_{g\,E_t}$ or $C_{g\,D} - C_{g\,g_c}$ indicates that E_t or g_c was centered more towards the morning than D while a positive $C_{g\,D} - C_{g\,E_t}$ or $C_{g\,D} - C_{g\,g_c}$ indicates that E_t or g_c was centered more towards the afternoon than D. $C_{g\,D} - C_{g\,E_t}$ or $C_{g\,D} - C_{g\,g_c}$ would be zero if the diurnal patterns of D and E_t or D and g_c were centered at a similar point (but not necessarily at noon). At the lowest soil moisture levels (<15% by volume at 10 cm) both weekly mean $C_{g\,D} - C_{g\,E_t}$ and $C_{g\,D} - C_{g\,g_c}$ were the most negative, ranging from −0.55 to −0.12 for $C_{g\,D} - C_{g\,E_t}$ and −1.3 to −0.7 for $C_{g\,D} - C_{g\,g_c}$. For soil moisture levels at 10 cm between 15 and 25% the weekly mean $C_{g\,D} - C_{g\,E_t}$ was fairly stable at −0.2 to −0.1 (with one point at 0.13). $C_{g\,D} - C_{g\,g_c}$ for soil moisture levels between 15 and 25% was more variable than $C_{g\,D} - C_{g\,g_c}$ with values between −1.2 and 0. Both $C_{g\,D} - C_{g\,E_t}$ and $C_{g\,D} - C_{g\,g_c}$ had positive and negative values for soil moisture levels of 25–30%. After soil moisture reached 30%, the majority of values for both $C_{g\,D} - C_{g\,E_t}$ and $C_{g\,D} - C_{g\,g_c}$ were positive. $C_{g\,D} - C_{g\,E_t}$ had values ranging from −0.3 to +0.4 with 70% of the values >0 while $C_{g\,D} - C_{g\,g_c}$ had values ranging from −0.4 to 2.1 with 88% of the values >0 when soil moisture at 10 cm was greater than 30%.

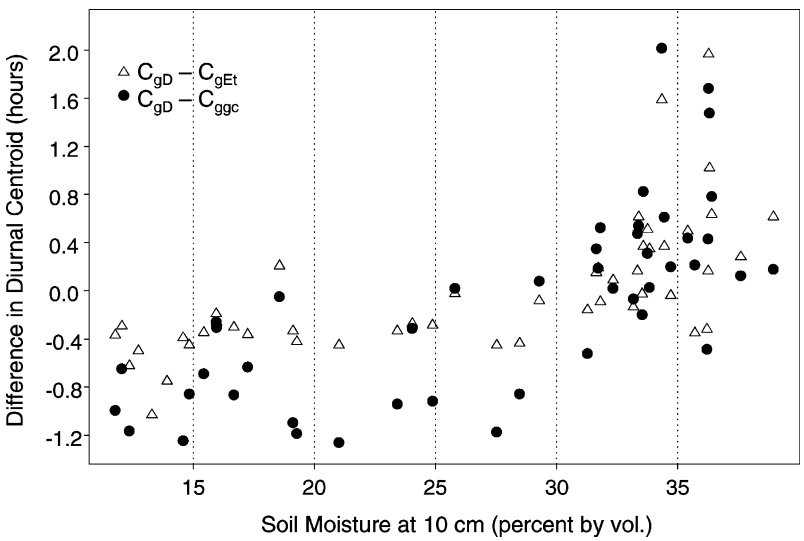

Fig. 7. Diurnal centroid of vapor pressure deficit minus diurnal centroid of transpiration ($C_{g\,D} - C_{g\,E_t}$) and diurnal centroid of vapor pressure deficit minus diurnal centroid of canopy conductance ($C_{g\,D} - C_{g\,g_c}$) vs. soil moisture at 10 cm.

The daytime pattern of summer water potential show that the trees experienced daily water stress (Table 3). Ponderosa pine trees close their stomata when the water potential decreases below −1.65 to −2.0 MPa (DeLucia et al., 1988; Running, 1976): this occurred in late afternoon even when the pre-dawn water potential showed that the trees were not yet chronically water stressed.

4. Discussion

4.1. Seasonal patterns

During the summer and fall transpiration (E_t) and soil evaporation (E_s) contributed equally to evapotranspiration (E) whereas E_t was the dominant water flux (>70% of E) in winter and spring. E_t was high in the summer and early fall, decreased through late fall to a minimum in winter, then increased again to a maximum in late spring. Irvine et al. (2002) reported summer E_t rates at a young (14 years old) ponderosa pine plantation in central Oregon with LAI of 1.0 to be ∼1.0 mm day^{-1}. Therefore, these two sites had similar E_t rates per unit leaf area during the summer. Daily E_t rates indicate that the trees do not become truly dormant in winter and are active when daytime mean air temperatures exceed 4–5 °C. Daily E_t rates also show that the trees can maintain high levels of E_t through the summer despite little or no rainfall. The onset of the rainy period did not cause increased E_t likely due to the colder air temperatures and lower Q_p that accompanied the precipitation. The highest E_t rates occurred in late spring at the end of the rainy season: during this period soil moisture was high concurrent with high Q_p, air temperature, and D. E_s was highest in the summer and lowest in the winter with moderate levels in both fall and spring. While E_s decreased similarly to E_t during the onset of the rainy period, it did not increase as quickly as E_t at the transition from rainy to dry season. Canopy conductance (g_c) was low in the summer when soil moisture was limiting and D was high and then increased in the fall as D decreased. During the winter g_c was moderate and highly variable. Canopy conductance (g_c) increased substantially at the beginning of March—this period had high soil moisture, moderately high Q_p, and low D. Canopy conductance (g_c) decreased in late spring as the hot and dry conditions of the summer began to prevail.

4.2. Diurnal patterns

Mean diurnal cycles for E_t and g_c during the drought period showed an early morning spike, an afternoon depression, and a mid-late afternoon sub-peak. These features are likely related to the specific strategy of water use for these trees during drought. Light intensity is maximal at noon while D is maximal later in the afternoon; therefore, the optimal daily time course of stomatal opening during drought is to allow photosynthesis during the morning hours, and to close the stomata in the afternoon (Makela et al., 1996). The early morning spike in E_t was the result of high g_c during a period of the day when xylem water potential is least negative, light was sufficient for photosynthesis, and the evaporative demands low. Soil water potential data indicate that the trees became drought stressed throughout the summer in mid-day, resulting in stomatal closure and the observed mid-day depression in E_t. A mid-day depression in stomatal conductance has been observed by Pataki et al. (1998), Teixeira Filho et al. (1998), Tenhunen et al. (1981, 1982), and Lange et al. (1982). Tenhunen et al. (1981, 1982) and Lange et al. (1982) considered the mid-day depression to be a characteristic of Mediterranean species that allows them to reduce water losses when the evaporative demand is highest. Further, they believe that it is probably controlled by the saturation vapor pressure deficit of the air. Alternative explanations have been put forth by Hinckley et al. (1978) who suggested that it depends on a combination of several factors and especially the instantaneous water potential and Correia et al. (1990) who suggested that it results from the inhibitory effects of intense photosynthetic radiation on the chloroplasts.

The afternoon peak in E_t during the drought likely occurred after partial recovery in water status following the afternoon stomatal closure: this period represents an additional time of sufficient light for photosynthesis with decreasing D. According to Irvine et al. (1998) the partial recovery of stomatal conductance, which would allow increased transpiration later in the day, is rarely reported in the literature for coniferous species but is apparent in data presented for *Pinus pinaster* (Loustau et al., 1996) and for *Pinus sylvestris* (Irvine et al., 1998). It is interesting

that the pattern of afternoon peaks in g_c occurred in summer, winter, and spring—this includes periods of active E_t and periods of both high and low water availability. This pattern suggests that the transport of water from roots to leaves is not fast enough to allow continuously high rates of E_t even when soil moisture levels are not limiting.

4.3. Strategy of water use

Ponderosa pine trees in the Sierra Nevada Mountain must contend with hot, dry, and sunny summers and near-freezing, wet, and cloudy winters. Summer E_t is therefore limited by drought while winter E_t is limited by low air temperature and low Q_p. We observed a general strategy of water use by ponderosa pine in which the trees maximize stomatal conductance and fixation of carbon throughout the day on warm sunny days with high soil moisture (i.e. warm periods in winter and late spring). During the dry period the trees regulate water loss to maximize carbon fixation in the morning when D is low. Accordingly, we observed moderate rates of E_t during warm winter periods, the highest E_t rates for the year in late spring, and high but slightly declining E_t rates through summer into fall.

A critical aspect of the strategy of water use is the ability to regulate water use throughout the summer to allow high carbon fixation despite low soil availability. Makela et al. (1996) determined a theoretical solution for the response of E_t to drought based on the amount of water available in the soil and the probability of rain in a climate to which the plant is adapted. In an area with a low probability of rain, the optimal E_t rate should be slow and steady to endure the drought period. Under the typical conditions of very little rain during the summer months in the Sierra Nevada Mountains, the ponderosa pine trees were found to be very successful at regulating water loss to maintain a fairly constant, slightly decreasing rate of water loss all summer, even during periods of measured drought stress. This constant E_t was maintained through the tight coupling of the stoma to the air conditions (Ω factor of 0.2–0.3 over the year) (Hollinger et al., 1994). Ω is a dimensionless factor with values between 0 and 1 that describes how coupled the saturation deficit at the leaf surface is to that of the air outside the leaf boundary layer (Jarvis and McNaughton, 1986). A tight coupling of the stomata to air conditions (i.e. lower Ω) indicates that stomatal conductance is strongly related to D. Therefore, these data suggest that during the dry summer the ponderosa pine trees at this site moderate the timing of stomatal opening/closure to maintain a constant daily rate of E_t given changing D and air temperature.

The traditional feed-forward model of stomatal response to D (Farquhar, 1978)—in which stomatal conductance declines before any adverse effects of water shortage arise in the leaves—does not seem to apply to ponderosa pine trees at our site. In a feed-forward situation, where stomata respond directly to humidity without regard to changes in E_t, E_t would decrease at high levels of D. In contrast, in a feedback situation, increases in D cause an initial increase in E_t, resulting in a decrease in leaf water potential. Stomata close due to lowered soil water potential which results in a negative feedback effect on E_t. The feedback scenario is characterized by an increase in E_t that levels off with increasing D as was observed in this study. While we did see evidence of partial stomatal closure in mid-afternoon when D was high, this was more likely a feedback mechanism responding to low leaf water potential. Lack of decreasing E_t rates at high D (Farquhar, 1978) was also reported by Pataki et al. (1998) (*Pinus taeda*) and Irvine et al. (1998) (*P. sylvestris*).

It has been proposed that the strategy of water use depends on the availability of water in the soil and therefore changes dynamically over a period of drought (Makela et al., 1996). Since the water status of a plant is influenced by both water content in the air (D) and water in the soil (soil moisture) we would expect both D and soil moisture to play a role in the strategy of water use; however, it is not clear how E_t responds to the combined effects of D and soil moisture. Further, despite known drought conditions at our site we have not observed a strong direct response of E_t to changes in soil moisture. At this site we previously found that the trees begin to show effects of severe drought only after soil moisture has dropped below ~12% in the top 20 cm (Bauer et al., 2000). Similarly, in an investigation of the impact of drought on the physiology of Scots pine (*P. sylvestris*) in central Scotland, Irvine et al. (1998) found that E_t in the drought treatment remained largely unaffected until soil moisture in the top 20 cm fell below ~12%. Wilson et al. (2001) reported a similar finding: during

pre-drought and moderate drought, water fluxes responded similarly to D while daytime mean soil moisture was not found to influence E_t rates. Our work corroborates the findings that changes in soil moisture do not produce linear changes in E_t rates. However, this does not mean the role of soil moisture is unimportant in determining water use patterns. Our results show that the diurnal patterns of E_t and g_c were affected by soil moisture. Specifically, a diurnal centroid analysis of E_t, g_c, and D suggests that the effect of soil moisture is to influence the timing of peak E_t and g_c relative to peak D. Periods of high soil moisture typically occurred during cold, rainy periods. During these periods E_t and g_c were maximized at similar times to maximum D, which is generally coincident with maximum air temperatures. When soil moisture levels were low E_t rates and g_c were centered towards the morning while D was centered towards the afternoon. Therefore during drought periods the strategy of water use was to maximize E_t (and so carbon fixation) in the morning when D was low.

4.4. Model and methodology comparison

The FORFLUX model results agreed well in both magnitude and pattern with daily total E_t. Modeled E_t agreed well with measured E_t during the dry period but underestimated E_t during the rainy period. We conclude that FORFLUX was able to simulate the strategy for water regulation through the dry period, including during moderate drought stress. However, FORFLUX did not capture the ability of the trees to transpire during the winter during warmer periods nor did it predict the high E_t rates observed in mid-spring. At the lowest levels of Q_p and air temperature, the modeled and measured E_t were similarly low. However, the model responded differently than actual E_t to the mid-ranges of Q_p and air temperature. Once air temperature and Q_p reach levels greater than 5 °C and 300 μmol m^{-2} s^{-1}, respectively, the trees had a higher capacity to transpire than predicted by the model. If part of the strategy of water use for ponderosa pine trees at our site is to maintain activity in the winter and spring when soil moisture levels are high, as we have suggested, the trees must be active at moderately low Q_p and air temperatures. Therefore, while FORFLUX was able to simulate water use for ponderosa pine specifically during the drought period, it did not simulate the entire seasonal activity of this drought-adapted species.

Modeled E_s agreed in magnitude with $E - E_t$ and sub-canopy measurements of E_s but the variability was only moderately correlated with $E - E_t$. Modeled E_s was similar in magnitude to $E - E_t$ during the dry season but slightly higher during the rainy period. Since all measures of soil evaporation were coarse estimates we can qualitatively compare the performance of FORFLUX to the calculated/measured values but cannot determine how well FORFLUX simulated actual soil evaporation. Modeled E_t and E_s were both most similar to measured/calculated values during the dry season which produced good agreement in E during the period. The model overestimated E_s and underestimated E_t during the rainy season. The high model estimate of E_s compensated for the low model estimate of E_t resulting in good agreement between modeled and measured E during this period.

5. Conclusion

The partitioning of water fluxes changed dynamically over the year. Water fluxes were partitioned equally between transpiration and soil evaporation during the summer and fall while transpiration was the dominant water flux in winter and spring. The FORFLUX model generally captured the year-round trends in water fluxes but performed better in the dry period (including during the drought period) than in the wet period. On a seasonal timescale, the general strategy of water use we observed showed that the trees take advantage of warm sunny periods with high soil moisture (i.e. warm periods in winter and late spring) to maximize stomatal aperture and thus carbon fixation throughout the day, but regulate water loss to maximize carbon fixation in the morning while minimizing water loss through the dry periods. The trees had high rates of transpiration in the early morning and mid-late afternoon, with a mid-day depression in transpiration during the drought period. While we believe this diurnal pattern to be driven by a combination of xylem water potential, Q_p, and D, more research is needed to examine the multiple hypotheses for this observed pattern. Despite becoming moderately drought stressed, transpiration rates were not directly affected by low soil moisture levels. A

diurnal centroid analysis revealed that the effect of soil moisture on transpiration was to influence the timing of high transpiration relative to high *D*. Finally, we observed the stomatal response to *D* to be feedback driven, rather than following the traditional feed-forward model of stomatal response to *D*.

Acknowledgements

This research was funded by the Environmental Protection Agency Science to Achieve Results (STAR), Ecosystem Indicators Program (award R826601); and University of California Agricultural Experiment Station. We thank Bob Heald and the Blodgett Forest crew, and Gunnar Schade for their invaluable support in field setup and maintenance. This work could not have been possible without the generous guidance by Steve Burgess, Tim Bleby, and Todd Dawson. We also thank Sierra Pacific Industries for use of their land and assistance in field site operations.

References

Baker, B., Guenther, A., Greenberg, J., Goldstein, A., Fall, R., 1999. Canopy fluxes of 2-methyl-3-buten-2-ol over a ponderosa pine forest by relaxed eddy accumulation: field data and model comparison. J. Geophys. Res. Atmos. 104, 26107–26114.

Baldocchi, D.D., Verma, S.B., Anderson, D.E., 1987. Canopy photosynthesis and water-use efficiency in a deciduous forest. J. Appl. Ecol. 24, 251–260.

Ball, J.T., Woodrow, I.E., Berry, J.A., 1987. A model predicting stomatal conductance and its contribution to the control of photosynthesis under different environmental conditions. In: Biggens, J. (Ed.), Progress in Photosynthesis Research. Martinus Nijhoff Publishers, Dordrecht, pp. 221–224.

Ball, J.T., Woodrow, I.E., Berry, J.A., 1988. A model predicting stomatal conductance and its contribution to the control of photosynthesis under different environmental conditions. In: Biggens, J. (Ed.), Progress in Photosynthetic Research. Mirtinus Nijhoff Publishers, The Netherlands, pp. 221–224.

Bauer, M.R., Hultman, N.E., Panek, J.A., Goldstein, A.H., 2000. Ozone deposition to a ponderosa pine plantation in the Sierra Nevada Mountains (CA): a comparison of two different climatic years. J. Geophys. Res. 105 (17), 22123–22136.

Becker, P., Edwards, W.R.N., 1999. Corrected heat capacity of wood for sap flow calculations. Tree Physiol. 19 (11), 767–768.

Brooks, A., Farquhar, G.D., 1985. Effects of temperature on the CO_2/O_2 specificity of ribulose-1,5-bisphosphate carboxylase/oxygenase and the rate of respiration in the light. Planta 165, 397–406.

Burgess, S.S.O., et al., 2001. An improved heat pulse method to measure low and reverse rates of sap flow in woody plants. Tree Physiol. 21, 589–598.

Campbell, G.S., 1977. An Introduction to Environmental Biophysics. Springer, New York, p. 155.

Chambers, S.D., Hacker, J.M., Williams, A.G., 1997. RAMF Version 8.1 User's Manual, vol. 14, 2nd ed. Flinders University of South Australia, Adelaide, Australia.

Clearwater, M.J., Meinzer, F.C., Andrade, J.L., Goldstein, G., Holbrook, N.M., 1999. Potential errors in measurement of nonuniform sap flow using heat dissipation probes. Tree Physiol. 19 (10), 681–687.

Collatz, G.J., Ball, J.T., Grivet, C., Berry, J.A., 1991. Physiological and environmental regulation of stomatal conductance, photosynthesis and transpiration: a model that includes a laminar boundary layer. Agric. Forest Meteorol. 54, 107–136.

Correia, M.J., Chaves, M.J., Pereira, J.S., 1990. Afternoon depression in photosynthesis in grapevine leaves. Evidence for a high light stress effect. J. Exp. Bot. 41, 417–426.

DeLucia, E.H., Schlesinger, W.H., Billings, W.D., 1988. Water relations and the maintenance of Sierran conifers on hydrothermally altered rock. Ecology 69, 303–311.

Dye, P.J., Olbrich, B.W., Poulter, A.G., 1991. The influence of growth rings in *Pinus patula* on heat pulse velocity and sap flow measurement. J. Exp. Bot. 42, 867–870.

Farquhar, G.D., 1978. Feedforward responses of stomata to humidity. Aust. J. Plant Physiol. 5, 787–800.

Farquhar, G.D., 1988. Models relating subcellular effects of temperature to whole plant responses. In: Long, S.P., Woodward, F.I. (Eds.), Plants and Temperature. Society for Experimental Biology, University of Cambridge, Cambridge, pp. 395–409.

Farquhar, G.D., Song, S.C., 1984. An empirical model of stomatal conductance. Aust. J. Plant Physiol. 11, 191–210.

Farquhar, G.D., von Caemmerer, S., 1982. Modeling of photosynthetic response to environmental conditions. In: Lange, O.L., Nobel, P., Osmond, C.B., Ziegler, H. (Eds.), Physiological Plant Ecology. II. Water Relations and Carbon Assimilation. Springer, Berlin, pp. 549–587.

Farquhar, G.D., von Caemmerer, S., Berry, J.A., 1980. A biochemical model of photosynthetic CO_2 assimilation in leaves of C_3 species. Planta 149, 78–90.

Gates, D.M., 1980. Biophysical Ecology. Springer, New York, p. 611.

Goldstein, A.H., et al., 2000. Effects of climate variability on the carbon dioxide, water, and sensible heat fluxes above a ponderosa pine plantation in the Sierra Nevada (CA). Agric. Forest Meteorol. 101, 113–129.

Granier, A., 1987. Evaluation of transpiration in a Douglas-fir stand by means of sap flow measurements. Tree Physiol. 3, 309–320.

Granier, A., Loustau, D., 1994. Measuring and modelling the transpiration of a maritime pine canopy from sap-flow data. Agric. Forest Meteorol. 71 (1/2), 61–81.

Harley, P.C., Thomas, R.B., Reynolds, J.F., Strain, B.R., 1992. Modelling photosynthesis of cotton grown in elevated CO_2. Plant Cell Environ. 15, 271–282.

Hatton, T.J., Vertessy, R.A., 1989. Variability of sap flow in *Pinus radiata* plantation and the robust estimation of transpiration.

In: Hydrology and Water Resources Symposium. Australian Institution of Engineers, Christchurch, New Zealand, pp. 6–10.
Hatton, T.J., Vertessy, R.A., 1990. Transpiration of plantation *Pinus radiata* estimated by the heat pulse method and the Bowen ratio. Hydrol. Processes 4, 289–298.
Hatton, T.J., Catchpole, E.A., Vertessy, R.A., 1990. Integration of sap flow velocity to estimate plant water use. Tree Physiol. 6, 201–209.
Hatton, T.J., Moore, S.J., Reece, P.H., 1995. Estimating stand transpiration in a *Eucalyptus populnea* woodland with the heat pulse method: measurement errors and sampling strategies. Tree Physiol. 15, 219–227.
Hinckley, T.M., Duhme, F., Hinckley, A.R., Richter, H., 1978. Drought relations of shrub species: assessment of the mechanism of drought resistance. Oecologia 59, 344–350.
Hollinger, D.Y., Kelliher, F.M., Schulze, E.D., Kostner, B.M.M., 1994. Coupling of tree transpiration to atmospheric turbulence. Nature 371 (6492), 60–62.
Irvine, J., Perks, M.P., Magnani, F., Grace, J., 1998. The response of *Pinus sylvestris* to drought: stomatal control of transpiration and hydraulic conductance. Tree Physiol. 18 (6), 393–402.
Irvine, J., Law, B.E., Anthoni, P.M., Meinzer, F.C., 2002. Water limitations to carbon exchange in old-growth and young ponderosa pine stands. Tree Physiol. 22, 189–196.
Jarvis, P.G., McNaughton, K.G., 1986. Stomatal control of transpiration: scaling up from leaf to region. Adv. Ecol. Res. 15, 1–49.
Kaimal, J.C., Finnegan, J.J., 1994. Atmospheric Boundary Layer Flows—Their Structure and Measurement. Oxford University Press, New York, p. 289.
Kline, J.R., Reed, K.L., Waring, R.H., Stewart, M.L., 1976. Field measurement of transpiration in Douglas-fir. J. Appl. Ecol. 13, 272–283.
Kostner, B., Granier, A., Cermak, J., 1998. Sapflow measurements in forest stands: methods and uncertainties. Annales Des Sciences Forestieres 55 (1/2), 13–27.
Lamanna, M., Goldstein, A.H., 1999. In situ measurements of C2–C10 VOCs above a Sierra Nevada pondersa pine plantation. J. Geophys. Res. 104, 21247–21262.
Lange, O.L., Tenhunen, J.D., Braun, M., 1982. Midday stomatal closure in Mediterranean-type scleropylls under simulated habitat conditions in an environmental chamber. I. Comparison of the behavior of various Mediterranean species. Flora 172, 563–579.
Lassoie, J.P., Scott, D.R.M., Fritschen, I.J., 1977. Transpiration studies in Douglas-fir using the heat pulse technique. Forest Sci. 23, 377–390.
Law, B.E., Williams, M., Anthoni, P.M., Baldocchi, D.D., Unsworth, M.H., 2000. Measuring and modelling seasonal variation of carbon dioxide and water vapour exchange of a *Pinus ponderosa* forest subject to soil water deficit. Global Change Biol. 6 (6), 613–630.
Leuning, R., Judd, M.J., 1996. The relative merits of open- and closed-path analysers for measurement of eddy fluxes. Global Change Biol. 2, 241–253.
Loustau, D., et al., 1996. Transpiration of a 64-year-old maritime pine stand in Portugal. Seasonal course of water flux through maritime pine. Oecologia 107, 33–42.
Makela, A., Berninger, F., Hari, P., 1996. Optimal control of gas exchange during drought—theoretical analysis. Ann. Bot. 77 (5), 461–467.
McMillen, R.T., 1988. An eddy correlation technique with extended applicability to non-simple terrain. Boundary-Layer Meteorol. 43, 231–245.
Miller, D.R., Vavrina, C.A., Christensen, T.W., 1980. Measurement of sap flow and transpiration in ring-porous oaks using the heat pulse velocity technique. Forest Sci. 19, 291–296.
Monteith, J.L., Unsworth, M.H., 1990. Principles of Environmental Physics. Edward Arnold, London, p. 291.
Nikolov, N.T., 1997a. Mathematical Modeling of Seasonal Biogeophysical Interactions in Forest Ecosystems. Dissertation Thesis, Colorado State University, Fort Collins, p. 149.
Nikolov, N.T., 1997b. Modeling Spatial Distribution of Leaf Area Index, Canopy Conductance to Ozone, and Fluxes of CO_2, O_3, and Latent Heat at the San Joaquin Valley (CA). USDA FS, Fort Collins, CO.
Nikolov, N.T., Massman, W.J., Schoettle, A.W., 1995. Coupling biochemical and biophysical processes at the leaf level: an equilibrium photosynthesis model for leaves of C_3 plants. Ecol. Model. 80, 205–235.
Olbrich, B.W., 1991. The verification of the heat pulse technique for estimating sap flow in *Eucalyptus grandis*. Can. J. Forest Res. 21, 836–841.
Pataki, D.E., Oren, R., Katul, G., Sigmon, J., 1998. Canopy conductance of *Pinus taeda*, *Liquidambar styraciflua* and *Quercus phellos* under varying atmospheric and soil water conditions. Tree Physiol. 18 (5), 307–315.
Rissmann, J., Tetzlaff, G., 1994. Application of a spectral correction method for measurements of covariances with fast-response sensors in the atmospheric boundary layer up to a height of 130 m and testing of the corrections. Boundary-Layer Meteorol. 70, 293–305.
Running, S.W., 1976. Environmental control of leaf water conductance in conifers. Can. J. Forest Res. 6, 104–112.
Saugier, B., Granier, A., Pontailler, J.Y., Dufrene, E., Baldocchi, D.D., 1997. Transpiration of a boreal pine forest measured by branch bag, sap flow and micrometeorological methods. Tree Physiol. 17, 511–519.
Sharkey, T.D., 1985. Photosynthesis in intact leaves of C_3 plants: physics, physiology and rate limitations. Bot. Rev. 51, 53–105.
Shuttleworth, W.J., et al., 1984. Eddy correlation measurements of energy partition for Amazonian forest. Q. J. R. Meteorol. Soc. 110, 1143–1162.
SNEP, 1996. Status of the Sierra Nevada: Assessment Summaries and Management Strategies, vol. 36. Wildland Resources Center, Davis.
Tardieu, F., Davies, W.J., 1993a. Integration of hydraulic and chemical signalling in the control of stomatal conductance and water status of droughted plants. Plant Cell Environ. 16, 341–349.
Tardieu, F., Davies, W.J. (Eds.), 1993b. Root–shoot communication and whole-plant regulation of water flux. In: Water Deficit. Plant Responses from Cell to Community. BIOS Sci. Publishers, Oxford, pp. 147–162.
Tardieu, F., Zhang, J., Gowing, D.J.G., 1993. Stomatal control by both (ABA) in the xylem sap and leaf water status: a test of a

model for droughted or ABA-fed field-grown maize. Plant Cell Environ. 16, 413–420.

Teixeira Filho, J., Damesin, C., Rambal, S., Joffre, R., 1998. Retrieving leaf conductances from sap flows in a mixed Mediterranean woodland: a scaling exercise. Annales Des Sciences Forestieres 55 (1/2), 173–190.

Tenhunen, J.D., Lange, O.L., Braun, M., 1981. Midday stomatal closure in Mediterranean type sclerophylls under simulated habitat conditions in an environmental chamber. II. Effects of the complex leaf temperature and air humidity on gas exchange of *Arbutus unedo* and *Quercus ilex*. Oecologia 50, 5–11.

Tenhunen, J.D., Lange, O.L., Jagner, D., 1982. The control by atmospheric factors and water stress of midday stomatal closure in *Arbutus credo* growing in natural macchia. Oecologia 55, 165–169.

Wilson, K.B., Hanson, P.J., Mulholland, P.J., Baldocchi, D.D., Wullschleger, S.D., 2001. A comparison of methods for determining forest evapotranspiration and its components: sap-flow, soil water budget, eddy covariance and catchment water balance. Agric. Forest Meteorol. 106, 153–168.

Wilson, K.B., et al., 2003. The diurnal centroid analysis of ecosystem energy and carbon fluxes at FLUXNET sites. Agric. Forest Meteorol. (in press).